Self-calibrated Microwave Characterization of High-speed Optoelectronic Devices by Heterodyne Spectrum Mapping

Shangjian Zhang, *Member, IEEE*, Chong Zhang, Heng Wang, Xinhai Zou, Yali Zhang, Yong Liu, *Senior Member, IEEE*, and John E. Bowers, *Fellow, IEEE*

***Abstract*—A four-in-one electrical method is proposed based on heterodyne spectrum mapping for self-calibrated frequency response measurements of high-speed semiconductor laser diodes, Mach-Zehnder modulators, phase modulators and photodetectors with a shared self-heterodyne interferometer. The self-heterodyne interferometer provides mapping of the desired optical spectrum components from the optical domain to electrical domain, and allows indirect but self-calibrated measurement of these optical spectra in the electrical domain. Frequency responses including modulation index of semiconductor laser diodes, half-wave voltage and chirp parameter of Mach-Zehnder modulators, half-wave voltage of phase modulators and responsivity of photodetectors are experimentally extracted with this method, and compared to the results obtained with conventional methods for accuracy.**

***Index Terms*—Electro-optic modulators, frequency response, microwave photonics, optical mixing, photodetectors, semiconductor lasers.**

I. INTRODUCTION

HIGH-SPEED optoelectronic devices like semiconductor laser diodes (LDs), optical modulators (MODs) and photodetectors (PDs) play essential roles in optical fiber communication or radio-over-fiber (ROF) systems. ROF techniques combine the benefits of optical and wireless communication, including large fiber bandwidth, low fiber attenuation, low complexity, and lower cost, etc., which are very promising for satellite communications, mobile radio communications, broadband access, mobile broadband system and wireless LAN[1]-[2]. In this applications, high-frequency modulation characteristics of LDs, MODs and PDs are critical to the precise electrical-to-optical or optical-to-electrical signal conversion, especially for wideband microwave applications [1]-[3].

A number of optical or electrical methods have been developed for measuring the frequency response of high-speed LDs or MODs, such as the optical spectrum analysis method [4]-[7], the swept frequency method [8]-[10], and the optical down-conversion method [11]. Approaches for measuring the frequency response of PDs include such as the pulse excitation method [12],[13], the intensity noise method [14],[15], the swept frequency method [8],[9], the harmonics analysis method [16]-[18], and the optical heterodyne method [19]-[22]. The optical method involves analyzing optical spectrum of modulated optical signals for measuring MODs with an optical spectrum analyzer (OSA), which was initially demonstrated for half-wave voltage measurement of Mach-Zehnder modulators (MZMs) and phase modulators (PMs) and later extended to directly modulated LDs [23],[24]. This method enables direct and calibration-free measurement of absolute frequency responses for LDs, MZMs and PMs in the optical domain. However, it is difficult to operate at the lower frequency regime (below GHz), due to the resolution of grating-based OSAs (about 0.01 nm at 1550 nm). The resolution could be improved by using a Brillouin-based OSA or a heterodyne-based OSA, nevertheless, it is hard to eliminate the linewidth effect of optical source, since the modulated optical spectrum depends on both the optical source and optical modulator. On the other hand, the optical methods for measuring PDs provide microwave-component-free optical stimulus. The intensity noise method generates an ultra-wideband optical stimulus based on the amplified spontaneous emission (ASE) beat noise; however it suffers from low frequency stability and poor signal-to-noise ratio (SNR) [22]. The optical heterodyne method is based on wavelength beating of a single or two tunable lasers, nevertheless, the resultant broadened linewidth and fluctuated power requires careful calibration [21], especially when high-resolution characterization is involved.

For high-resolution measurement, considerable effort has being consequently directed to the electrical domain, in which the swept frequency method is widely used for relative

This work was supported by the National Natural Science Foundation of China (grants 61377037, 61421002, 61435010), the Innovation Funds of Collaboration Innovation Center of Electronic Materials and Devices (ICEM2015-2001), Science Foundation for Youths of Sichuan Province (2016JQ0014), China Scholarship Council (201506075001).

S. Zhang, H. Wang, X. Zou, Y. Zhang, and Y. Liu are with the Collaboration Innovation Center of Electronic Materials and Devices, and State Key Laboratory of Electronic Thin Films and Integrated Devices, University of Electronic Science & Technology of China, Chengdu, 610054, P. R. China. (e-mail: sjzhang@uestc.edu.cn).

C. Zhang and J. E. Bowers are with Department of Electrical & Computer Engineering, University of California, Santa Barbara, Santa Barbara CA 93106, USA. S. Zhang is presently on sabbatical at University of California, Santa Barbara.

This article has been accepted for publication in a future issue of this journal, but has not been fully edited. Content may change prior to final publication. Citation information: DOI 10.1109/JLT.2017.2678978, Journal of Lightwave Technology

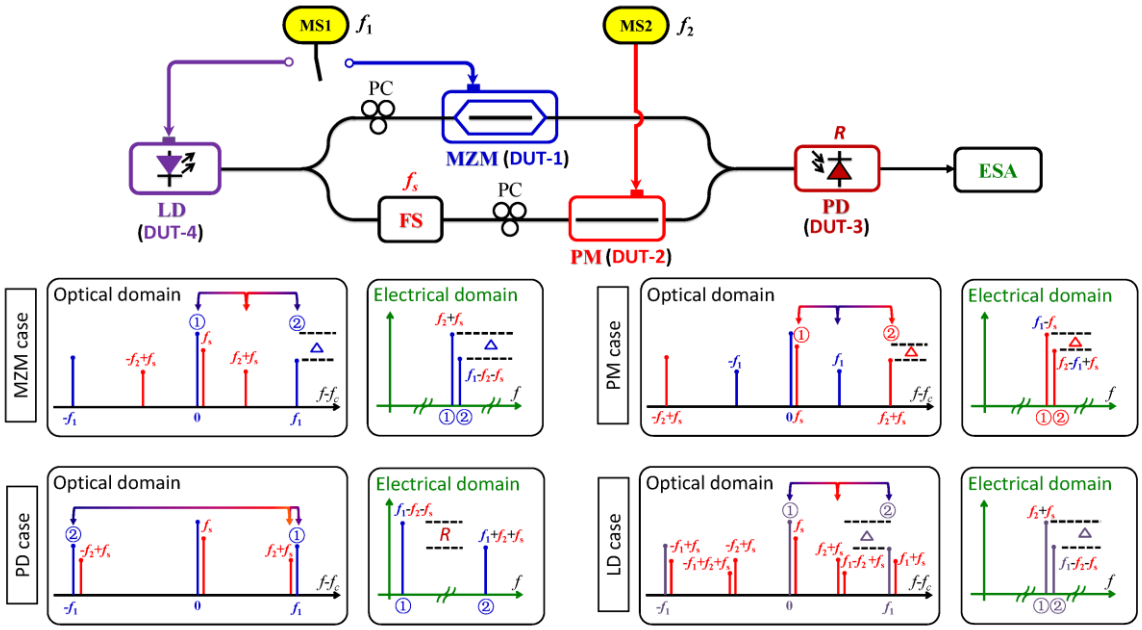

Fig. 1. Schematic setup of the proposed self-calibrated frequency response measurement method. LD, Laser diode, FS, Frequency shifter, MZM, Mach-Zehnder modulator, PM, Phase modulator, PD, Photodetector, PC, Polarization controller, ESA, Electrical spectrum analyzer, MS, Microwave source. The insets show the equivalent spectrum mapping from optical domain to electrical domain for every device under test.

frequency response measurement of LDs, MODs and PDs with the help of a vector network analyzer (VNA) or a lightwave component analyzer (LCA) [9]. The VNA-based method requires a wideband calibrated PD to characterize a LD or a MOD under test, or a wideband calibrated MZM to characterize a PD under test, and so it relies on de-embedding the assistant PD or MOD, since the measured total frequency response depends on both the test device and the assistant device. An improved swept frequency method was proposed for simplifying the calibration by using an electro-absorption modulator (EAM), in which the same EAM is assumed to feature identical responsivity when used as a MOD and a PD [10], which is not always valid. A major difficulty of the VNA-based method lies in the requirement of absolute responsivity of the assistant device, if absolute frequency response of the test device is needed. As we know, the absolute frequency response is more comprehensive than a relative one, since it reflects not only the relative change of modulation efficiency but also the modulation efficiency itself. Note that the relative frequency response can be easily obtained from the absolute one, but not vice versa. So, electrical methods that are capable of absolute frequency response measurement for optoelectronic devices with high resolution, and free of any extra calibration for the assistant devices are of great importance.

Recently, we demonstrated an electrical method for measuring the frequency response of PMs and PDs, respectively [25]-[27], by using optical frequency shifting and two-tone modulation, which eliminates correcting the responsivity fluctuation of assistant devices though a closely spaced two-tone modulation. In this paper, we proposed a four-in-one method based on heterodyne spectrum mapping for self-calibrated frequency response measurements of high-speed optoelectronic devices with a shared self-heterodyne interferometer. The interferometer consists of a LD, a MZM, a PM and a PD as well as a frequency shifter (FS), with which the desired optical carrier and sideband are mapped from optical domain to electrical domain, allowing to equivalently observe these optical spectrum lines in the electrical domain. We report for the first time a self-calibrated electrical method for measuring the absolute frequency responses for a LD, a MZM, a PM, and a PD with a single test setup, and calibration-free simultaneous measurement of modulation index, half-wave voltage and chirp parameter of a MZM by using electrical domain technique. A theoretical description is presented to fully explain our method as well as the experimental demonstration. Frequency responses including the modulation index of LDs, modulation index, half-wave voltage and chirp parameter of MZMs, modulation index and half-wave voltage of PMs, and responsivity of PDs are experimental measured, and the results are compared to those obtained using the conventional optical method to check the consistency and accuracy.

II. Theoretical Description

As shown in Fig. 1, the self-heterodyne interferometer consists of a LD, a MZM, a PM, a PD and a FS, where the MZM is located in the upper branch and the PM is located in the lower branch together with the FS. The interferometer is operated with the optical carrier at the frequency f_c from the LD and driven by two microwave signals $v_1(t)=V_1 sin(2\pi f_1 t)$ and $v_2(t)=V_2 sin(2\pi f_2 t)$. In the cases of MZM, PM and PD under test, the microwave signals are applied on MZM and PM, respectively, while in the case of LD under test, the microwave signals are applied on LD and PM, respectively. The output optical signal is collected by the PD and analyzed by an electrical spectrum analyzer (ESA).

This article has been accepted for publication in a future issue of this journal, but has not been fully edited. Content may change prior to final publication. Citation information: DOI 10.1109/JLT.2017.2678978, Journal of Lightwave Technology

In the upper branch of interferometer, the optical signal after MZM can be written as

$$E_z(t) = e^{j2\pi f_c t}\left[e^{jm_{z1}\sin(2\pi f_1 t)} + \gamma e^{jm_{z2}\sin(2\pi f_1 t)+j\varphi}\right] \quad (1)$$

where m_{zi} (i=1,2) are the modulation index corresponding to the upper or lower arm of the MZM, φ is the bias phase of MZM, and the asymmetric factor γ ($0\le\gamma\le1$) is splitting ratio of the two arms of MZM accounting for the infinite or finite ER (in dB) by ER=20*Log$_{10}$[(1+γ)/(1-γ)]. The modulation index and asymmetric factor of MZM can be determined from the conventional optical spectrum analysis by [5]

$$\frac{J_1(m_{zi})}{J_0(m_{zi})} = \frac{\sqrt{I_0(f_c+f_1)}-(-1)^i\sqrt{I_\pi(f_c+f_1)}}{\sqrt{I_0(f_c)}-(-1)^i\sqrt{I_\pi(f_c)}}, (i=1,2) \quad (2a)$$

$$\gamma = \frac{J_0(m_{z1})}{J_0(m_{z2})}\cdot\frac{\left[\sqrt{I_0(f_c)}-\sqrt{I_\pi(f_c)}\right]}{\left[\sqrt{I_0(f_c)}+\sqrt{I_\pi(f_c)}\right]}. \quad (2b)$$

where $I(f)$ is the optical spectrum power at frequency f, and the subscripts 0 and π denote the cases of bias phase φ=0 or π.

In the lower branch of interferometer, the optical signal after PM can be written by

$$E_p(t) = e^{j2\pi(f_c+f_s)t}e^{jm_p\sin(2\pi f_2 t)} \quad (3)$$

with the frequency f_s of FS. The modulation index m_p of PM can also be determined from optical spectrum analysis by [4]

$$\frac{J_1(m_p)}{J_0(m_p)} = \sqrt{\frac{I(f_c+f_s+f_2)}{I(f_c+f_s)}} \quad (4)$$

The intensity and phase modulated signal are combined and the generated photocurrent after PD can be accordingly written with the help of Jacobi-Anger expansion as [28]

$$\begin{aligned} i_\varphi(t)/R &= \left[1+\xi(t)\right]\left|E_z(t)+\eta E_p(t)e^{j\psi}\right|^2 = \left[1+\xi(t)\right]\cdot \\ &\left\{\begin{array}{l} 1+\gamma^2+\eta^2+2\gamma\sum_{k=-\infty}^{+\infty}J_k(m_{z1}-m_{z2})\cos(2\pi k f_1 t-\varphi)+2\eta\cdot \\ \sum_{k=-\infty}^{+\infty}\sum_{n=-\infty}^{+\infty}\left[J_k^2(m_{z1})+2\gamma J_k(m_{z1})J_k(m_{z2})\cos\varphi+\gamma^2J_k^2(m_{z2})\right]^{1/2} \\ \cdot J_n(m_p)\cos(2\pi k f_1 t-2\pi n f_2 t-2\pi f_s t-\psi) \end{array}\right\} \end{aligned} \quad (5)$$

with the responsivity R of PD, the microwave modulation signal $\xi(t)$ of LD, the relative amplitude η ($0\le\eta\le1$) and phase ψ of the two branches of interferometer, the kth and nth-order Bessel function $J_k(\cdot)$ and $J_n(\cdot)$ of the first kind (k,n=0, ±1, ±2,…).

MZM and PM cases

In the measurement of MZM and PM, the LD works as a continuous-wave optical source (i.e. $\xi(t)$ =0), while the MZM and the PM are modulated by the microwave signals at the frequencies f_1 and f_2, respectively. The electrical frequency components at kf_1-$nf_2\pm f_s$ can be quantified as following

$$\begin{aligned} i_\varphi(kf_1\pm nf_2\pm f_s) &= 2\eta\cdot R(kf_1\pm nf_2\pm f_s)\cdot J_n(m_p) \\ &\cdot\left[J_k^2(m_{z1})+2\gamma J_k(m_{z1})J_k(m_{z2})\cos\varphi+\gamma^2J_k^2(m_{z2})\right]^{1/2} \end{aligned} \quad (6)$$

In the case of MZM under test (DUT-1), the microwave frequency f_1 on the MZM is set close to twice of the microwave frequency f_2 on the PM ($f_1\approx2f_2>>f_s$), so that the assumption on the responsivity $R(f_1-f_2\pm f_s)\approx R(f_2\pm f_s)$ is satisfied. Thus, the modulation index and asymmetric factor of MZM can be extracted from

$$\begin{aligned} H_z(m_{z_i}) &= \frac{J_1(m_{zi})}{J_0(m_{zi})} = \frac{i_0(f_s)}{i_0(f_2\pm f_s)}\cdot \\ &\frac{\left[i_0(f_1-f_2\pm f_s)-(-1)^i i_\pi(f_1-f_2\pm f_s)\right]}{\left[i_0(f_s)-(-1)^i i_\pi(f_s)\right]}, (i=1,2) \end{aligned} \quad (7a)$$

and

$$\gamma = \frac{J_0(m_{z1})}{J_0(m_{z2})}\cdot\frac{\left[i_0(f_s)-i_\pi(f_s)\right]}{\left[i_0(f_s)+i_\pi(f_s)\right]}. \quad (7b)$$

The half-wave voltage and intrinsic chirp parameter of MZM can be accordingly solved by

$$V_\pi^z = \frac{\pi V_1}{m_{z1}-m_{z2}} \quad (8a)$$

$$\alpha = \frac{m_{z1}+\gamma^2 m_{z2}}{\gamma(m_{z1}-m_{z2})} \quad (8b)$$

In the case of PM under test (DUT-2), the microwave frequency f_2 on the PM is set close to twice of the microwave frequency f_1 on the MZM ($f_2\approx2f_1>>f_s$) so that the assumption of $R(f_2-f_1\pm f_s)\approx R(f_1\pm f_s)$ holds. So, the modulation index and half-wave voltage of PM can be determined by

$$H_p(m_p) = \frac{J_1(m_p)}{J_0(m_p)} = \frac{i_\varphi(f_2-f_1\pm f_s)}{i_\varphi(f_1\pm f_s)} \quad (9a)$$

$$V_\pi^p = \frac{\pi V_2}{m_p}. \quad (9b)$$

From Eqs. (2a), (2b), (7a) and (7b), the optical carrier at f_c and optical sideband f_c+f_1 are linearly mapped to electrical domain at frequencies $f_2\pm f_s$ and f_1-$f_2\pm f_s$, respectively, by setting the two microwave signals as $f_1\approx2f_2$. From Eqs. (4) and (9a), the optical carrier at f_c+f_s and optical carrier at f_c+f_s+f_1, are equivalently mapped to electrical domain at frequencies $f_1\pm f_s$ and f_2-$f_1\pm f_s$, respectively, by setting the two microwave signals as $f_2\approx2f_1$. Therefore, our method provides an equivalent electrical measurement of the desired optical carrier and intensity or phase modulated sideband in the electrical domain though the self-heterodyne spectrum mapping, and at the same time eliminates correcting responsivity fluctuation of the assistant devices by specially choosing the frequency relationship of two driving microwave signals. It is worthy noticing that our method allows the extraction of frequency response of MZM or PM at f_1 or f_2 from the desired electrical components at about f_1/2 or f_2/2, indicating the halved bandwidth requirement for the assistant devices. Moreover, our method works for the MZM with any ER, due to the inclusion of asymmetric factor for the infinite or finite ER of MZM.

This article has been accepted for publication in a future issue of this journal, but has not been fully edited. Content may change prior to final publication. Citation information: DOI 10.1109/JLT.2017.2678978, Journal of Lightwave Technology

PD case

In the case of PD under test (DUT-3), the electrical components at $f_1 \pm f_2 \pm f_s$, are investigated, which comes from sum-and-difference frequency of two pairs of optical intensity and phase modulated sidebands. As we know, each pair of optical sideband will keep equalized in optical domain, and their amplitude difference in the electrical domain only depends on the frequency response of PD, which can be seen from the common factor in Eq. (6) as $2\eta J_1(m_p)[J_1^2(m_{z1})+2J_1(m_{z1})J_1(m_{z2})cos\varphi+\gamma^2 J_1^2(m_{z2})]^{1/2}$. In the measurement, the microwave frequency f_1 on MZM is set close to the microwave frequency f_2 on PM ($f_1 \approx f_2 >> f_s$) and the lowest frequency f_1-$f_2 \pm f_s$ is fixed and close to DC. The responsivity of PD can be determined from the relative amplitude at $f_1+f_2 \pm f_s$ with respect to that at f_1-$f_2 \pm f_s$ by

$$R_f = \frac{R(f_1 + f_2 \pm f_s)}{R(f_1 - f_2 \pm f_s)} = \frac{i_\varphi(f_1 + f_2 \pm f_s)}{i_\varphi(f_1 - f_2 \pm f_s)}. \quad (10)$$

As the responsivity of the assistant MZM and PM is cancelled out, the frequency response of PD is self-calibrated measured in the electrical domain. It is noted that the desired heterodyning signals at $f_1 \pm f_2 \pm f_s$ hold a frequency span of about $2f_1$ or $2f_2$, indicating the doubled measuring frequency range.

LD case

In the case of LD under test (DUT-4), the LD and PM are driven by the microwave signals at the frequency f_1 and f_2, respectively, while the MZM is only biased with an appropriate DC voltage. In this case, the detected heterodyne signal after PD can be reorganized with the help of Jacobi-Anger expansion as [28]

$$i_\varphi(t)/R = \left[1+\mu_l \cos(2\pi f_1 t)\right] \cdot \left\{ \begin{array}{l} 1+\gamma^2+\eta^2+2\gamma\cos\varphi+2\eta\left(1+2\gamma\cos\varphi+\gamma^2\right)^{1/2} \\ \cdot \sum_{n=-\infty}^{+\infty} J_n(m_p)\cos\left[2\pi(nf_2+f_s)t+\psi-\varphi_x\right] \end{array} \right\} \quad (11a)$$

with

$$\varphi_x = arctan\left(\frac{\gamma \sin\varphi}{1+\gamma\sin\varphi}\right), \quad (11b)$$

the modulation index μ_l of LD at f_1. From Eq. (11a), the desired electrical components can be quantified in the frequency domain as following

$$\begin{aligned} &i_\varphi(nf_2 \pm f_s) = 2\eta \cdot \\ &R(nf_2 \pm f_s)\left(1+2\gamma\cos\varphi+\gamma^2\right)^{1/2} J_n(m_p) \end{aligned} \quad (12a)$$

and

$$\begin{aligned} &i_\varphi(f_1 \pm nf_2 \pm f_s) = \eta\mu_l \cdot \\ &R(f_1 \pm nf_2 \pm f_s)\left(1+2\gamma\cos\varphi+\gamma^2\right)^{1/2} J_n(m_p) \end{aligned} . \quad (12b)$$

The optical carrier at f_c and sideband at f_c+f_1 of LD are mapped into electrical domain at $f_2 \pm f_s$ and f_1-$f_2 \pm f_s$, respectively. For a self-calibrated measurement of LD, the microwave frequency f_1 is set close to twice of f_2 ($f_1 \approx 2f_2 >> f_s$) so that the term $R(f_1$-$f_2 \pm f_s)$ in Eq. (12a) can be considered equal to the term $R(f_2 \pm f_s)$ in Eq. (12b), and thus the modulation index μ_l of LD can be extracted by

$$\mu_l = 2\frac{i_\varphi(f_1 - f_2 \pm f_s)}{i_\varphi(f_2 \pm f_s)}. \quad (13)$$

From Eq. (13), the modulation index μ_l at f_1 is equivalently measured from the amplitude ratio between the desired electrical components at the frequencies $f_2 \pm f_s$ and f_1-$f_2 \pm f_s$ ($\approx f_1/2$), so our method halves bandwidth requirement for the assistant PM and PD.

From Eq. (5), (7)~(13), frequency responses of the MZM, PM, PD and LD can be independently measured with the self-heterodyne interferometer based on the heterodyne spectrum mapping, and the influence from other devices besides DUT is fully cancelled out by carefully choosing the frequency relationship between the two driving microwave signals. In the cases of MZM, PM and LD as DUT, the frequency response at f_1 or f_2 are extracted from the electrical spectra components at around $f_1/2$ or $f_2/2$, while in the case of PD as DUT, the frequency response at about f_1+f_2 is obtained with two driving microwave signal at f_1 and f_2, verifying the halved bandwidth requirement or the doubled measuring frequency range for the assistant devices. It is worthy noticing that our measurement is independent on the amplitude unbalance η and phase difference ψ of the self-heterodyne interferometer. The asymmetric factor γ and the phase bias φ of MZM will introduce same effect on the desired electrical components and will have little influence on the measured results. It is also noted that the phases of the two microwave signals will not affect the spectrum amplitudes of the desired electrical components, so it is not necessary to keep the two microwave signals synchronized, which makes the measurement simpler.

III. Experimental Demonstration

In the experiment, the optical carrier from a 1550 nm semiconductor LD is modulated by a $LiNbO_3$ MZM in the upper branch of interferometer. The same optical carrier is frequency-shifted by f_s=70 MHz with an acousto-optic FS (CETC YSG70) and then modulated by a PM in the lower branch of interferometer. The LD with a threshold current of 13.2 mA is biased at 30.2 mA with an output optical power of 1.5 mW. The MZM and PM are driven by two microwave sources (MS1, R&S SMB 100A; MS2, HP86320A), respectively. The output optical signal is detected by a PD and analyzed by an ESA (R&S FSU50). For an automatically swept measurement, the MS and ESA are controlled by a computer via NI-VISA bus. A MATLAB program is used to set the two MSs and acquire data from the ESA. For a better efficiency, two polarization controllers are used to align the polarization between two branches of interferometer. In order to reduce the residual reflection as much as possible, all the optical components are connected with angle polished (APC) finishes. It is noteworthy that the modulated signals in the upper or lower branch of interferometer are partially monitored by an OSA (YOKOGAWA AQ6370C) for the accuracy comparison.

This article has been accepted for publication in a future issue of this journal, but has not been fully edited. Content may change prior to final publication. Citation information: DOI 10.1109/JLT.2017.2678978, Journal of Lightwave Technology

In the MZM measurement, the driving microwave frequencies are set as $f_1=2f_2+0.02$ (GHz). The desired bias phases $\varphi=0$ or π are achieved by changing the applied bias voltage of MZM, where the maximum amplitude of $i(f_s)$ denotes the case of $\varphi=0$, and the minimum amplitude of $i(f_s)$ denotes the case of $\varphi=\pi$ according to Eq. (6). Figure 2(a) and 2(b) show typical heterodyne electrical spectra for $\varphi=0$ and π, respectively. In the case of f_1=16 GHz, f_2=7.99 GHz and f_s=70 MHz, the desired frequency components of 70 MHz (f_s), 7.92 GHz (f_2-f_s) and 7.94 GHz (f_1-f_2-f_s) are measured to be -14.91 dBm, -26.67 dBm and -57.93 dBm, respectively, for $\varphi=0$. And the desired frequency components of 70 MHz (f_s), 7.92 GHz (f_2-f_s) and 7.94 GHz (f_1-f_2-f_s) are measured to be -27.89 dBm, -39.66 dBm and -49.72 dBm, respectively, for $\varphi=\pi$. Therefore, the modulation index and asymmetric factor are determined to be m_{z1}=0.147, m_{z2}=-0.121 and γ=0.631 based on Eqs. (7a) and (7b), which corresponds to an intrinsic chirp parameter of 0.584 and a half-wave voltage of 8.91V at 16 GHz based on Eqs. (8a) and (8b). In our measurement, the ER of MZM is determined to be 12.91 dB by the obtained asymmetric factor γ of 0.631. It is

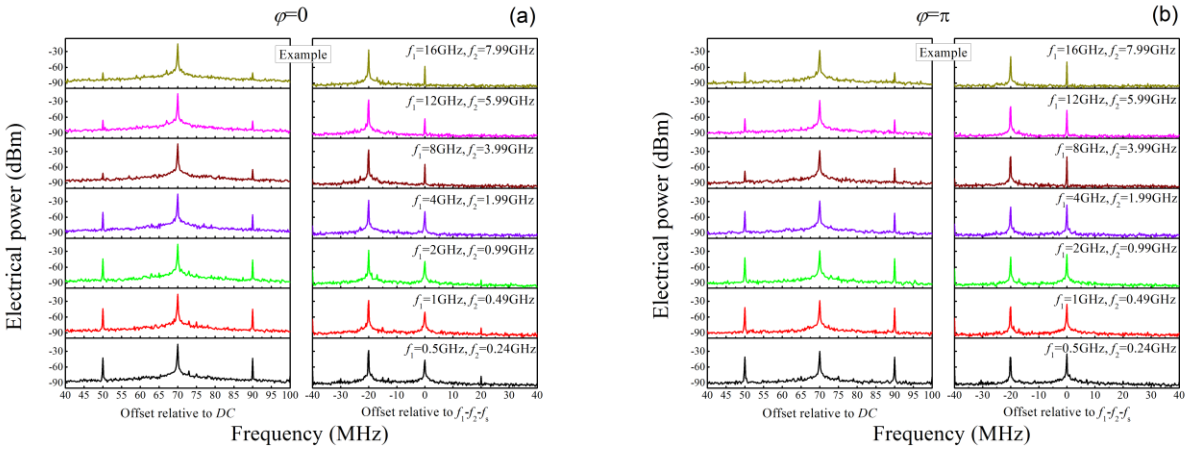

Fig. 2. Measured heterodyne spectra emphasized on the desired frequency components when (a) $\varphi=0$ and (b) $\varphi=\pi$, in the case of MZM under test.

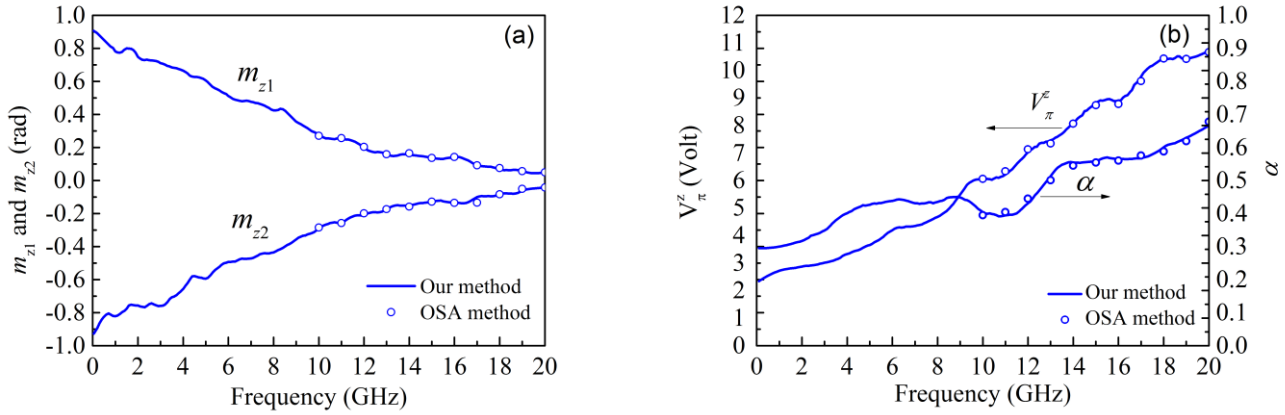

Fig. 3. (a) Modulation index and (b) half-wave voltage and chirp parameter measured with our method (solid lines) and with OSA method (open circles).

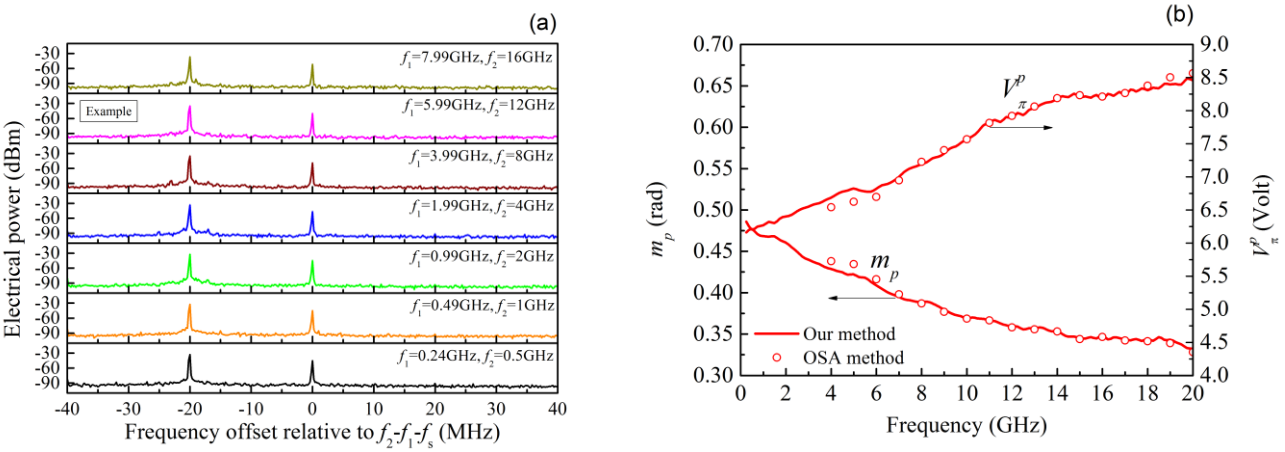

Fig. 4. Measured (a) electrical spectra emphasized on the desired frequency components, and (b) modulation index and half-wave voltage, in the case of PM under test, where the open circles represent the results with OSA method.

This article has been accepted for publication in a future issue of this journal, but has not been fully edited. Content may change prior to final publication. Citation information: DOI 10.1109/JLT.2017.2678978, Journal of Lightwave Technology

noteworthy that the measured frequency response at 16 GHz are extracted from the desired frequency components at about 8 GHz (7.92 GHz and 7.94 GHz), verifying the halved bandwidth requirement for the assistant PM and PD. The modulation index, half-wave voltages and chirp parameters are measured at different frequencies and illustrated as a function of frequency in Fig. 3(a) and 3(b).

In the PM measurement, the two microwave frequencies are set as $f_2=2f_1+0.02$ (GHz). Figure 4(a) shows several heterodyne electrical spectra emphasizing on the desired frequency components at f_1-f_s and f_2-f_1-f_s. For example, in the case of f_1=5.99 GHz and f_2=12 GHz, the modulation index and half-wave voltage of PM are solved to be m_p=0.359 rad and V_π^P=7.80 V at f_1=12 GHz, respectively, from the power ratio of -14.77 dB between electrical components at 5.92 GHz (f_1-f_s) and 5.94 GHz (f_2-f_1-f_s). The modulated index and half-wave voltage of PM at different frequencies are also measured and shown in Fig. 4(b).

In the PD measurement, the driving frequencies are set by $f_1=f_2+0.1$ (GHz). Figure 5(a) shows the heterodyne electrical spectra emphasizing on the desired frequency components at frequencies $f_1 \pm f_2$-f_s. For instance, in the case of f_1=6 GHz and f_2=5.9 GHz, the electrical powers at 11.83 GHz (f_1+f_2-f_s) is 5.02 dB lower than those at 30 MHz (f_1-f_2-f_s), and the frequency response R_f of PD are determined to be -5.02 dB at 11.83 GHz with respect to 30 MHz. The measurement can be easily swept to other frequency by simply changing the frequencies of two MS, and the frequency response of PD up to 20 GHz with respect to 30 MHz can be obtained, as shown in Fig. 5(b).

In the LD measurement, the two driving microwave frequencies are set as $f_1=2f_2+0.02$ (GHz). Figure 6(a) shows typical heterodyne electrical spectra emphasizing on the desired components at f_1-f_2-f_s and f_2-f_s. For example, the desired frequency components are measured to be -35.39 dBm at 5.92 GHz (f_2-f_s) and -65.54 dBm at 5.94 GHz (f_1-f_2-f_s), respectively, in the case of f_1=12 GHz and f_2=5.99 GHz, from which the heterodyne ratio is determined to be -30.17 dB. Therefore, the modulation index of LD at 12 GHz is solved to be 0.062 (μ_l) or -24.15 dB ($20\times Log_{10}\mu_l$). The measurement is swept to other frequencies, and the frequency-dependent modulation index is determined based on Eq. (13), as is shown in Fig. 6(b).

In the cases of MZM, PM and LD under test, the frequency responses are also measured by using conventional OSA-based method under the same driving level, and shown in Fig. 3(a), 3(b), 4(b) and 6(b) for comparison, where the lower measurable frequency of ~4 GHz (PM and LD cases) or ~10 GHz (MZM case) is limited by the resolution of OSA, since the best resolving wavelength (0.01 nm) can be achieved only when the two closed wavelengths are with the same amplitude according

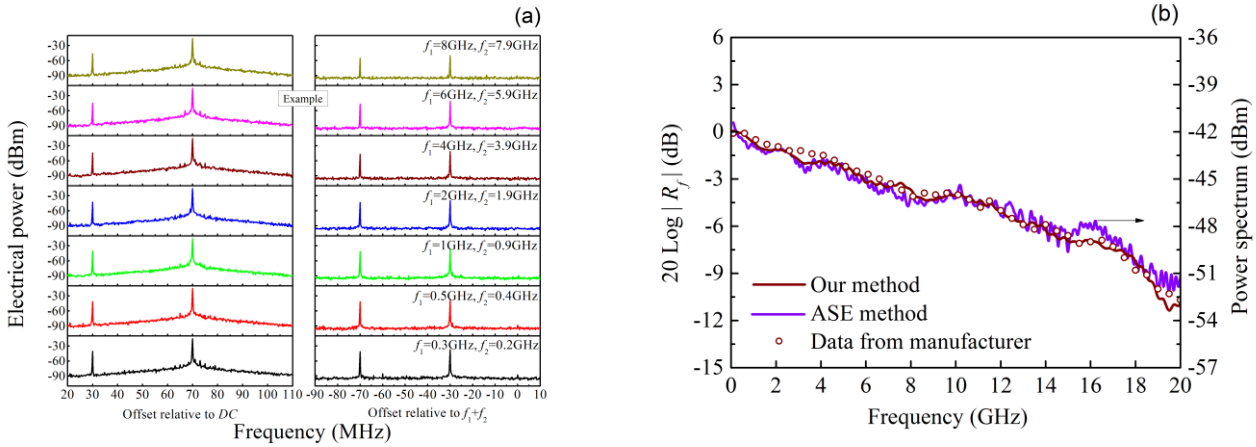

Fig. 5. Measured (a) electrical spectra emphasized on the desired frequency components, and (b) frequency response in the case of PD under test, where the results with ASE method (blue lines) and data from manufacturer (open circles) are included for comparison.

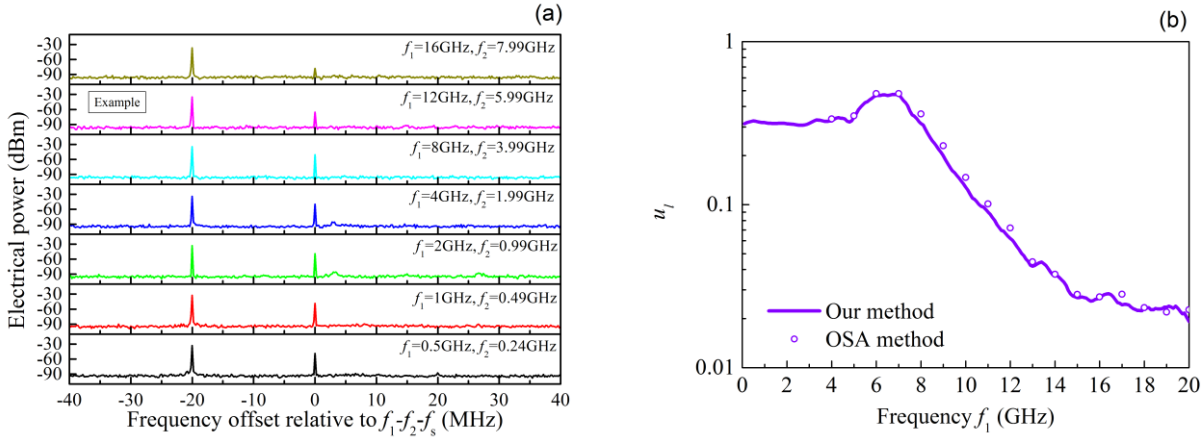

Fig. 6. Measured (a) electrical spectra emphasized on the desired frequency components, and (b) frequency response in the case of PD under test, where the results with ASE method (blue lines) and data from manufacturer (open circles) are included for comparison

This article has been accepted for publication in a future issue of this journal, but has not been fully edited. Content may change prior to final publication. Citation information: DOI 10.1109/JLT.2017.2678978, Journal of Lightwave Technology

to Rayleigh Criterion [25]. However, in our measurements, the desired optical spectra components are not with the same amplitude but a relative amplitude of $[J_1^2(m_{z1})+2J_1(m_{z1})J_1(m_{z2})cos\varphi \pm\gamma^2 J_1^2(m_{z2})]^{1/2}/[J_0^2(m_{z1})+2J_0(m_{z1})J_0(m_{z2})cos\varphi \pm\gamma^2 J_0^2(m_{z2})]^{1/2}$ (MZM case) or $J_1(m_p)/J_0(m_p)$ (PM case) or $2u_l$ (LD case), which explains why the best resolution cannot be guaranteed and the lower measurable frequency of optical spectrum analysis has to start from ~4 GHz or 10 GHz instead of ~1.2 GHz (0.01nm). Nevertheless, the good agreement between the measurable results indicates the equivalent spectra mapping from the optical domain to electrical domain, and our method does eliminate correcting the responsivity fluctuation of assistant devices, since the OSA method does not involve any assistant device. In the case of PD under test, our measured results are also compared to those obtained using the ASE method as well as the data provided by manufacturer, as shown in Fig. 5(b). All the measured results are in good agreement and coincide with the manufacturer data, verifying the self-calibrated frequency response measurement of PD.

The main limit, we think, comes from the SNR of the desired heterodyne electrical signals in our measurement. For the accuracy, it is practically recommended to know the bandwidth of the assistant devices before measurement. For example, if the measuring frequency range is 20 GHz for a MZM, it would be better to choose the assistant PM and PD with a bandwidth of beyond 10 GHz. Thanks to the self-calibration, the noise introduced by the 50 Ohm electrical ports can be cancelled when measuring the modulation index of MZM and PM. However, the noise will affect the accuracy of the half-wave voltage, because it will affect the measurement accuracy of the driving voltage and therefore the half-wave voltage of the modulator under test. If a device with unnegligible impedance mismatch is under test, the microwave driving voltage should be determined by taking into account the mismatch.

IV. Measurement Uncertainty

For the accuracy, we investigate the measurement uncertainty for every DUT. In our experiment, the uncertainty mainly comes from the error of electrical spectrum measurement, since our method is based on the electrical spectra analysis of heterodyne signals. Meanwhile, the uncertainty is also resulted by the assumption of $R(f_1-f_2-f_s)\approx R(f_2-f_s)$ in the case of the MZM, PM and LD under test.

In the MZM measurement, the error dependence of modulation index m_{zi} (i=1,2) on the heterodyning ratio H_z can be derived from the total derivative of Eq. (7a) or (7b), given by

$$\delta m_{zi}/m_{zi}=F_z\cdot\delta H_z/H_z=F_z\cdot \left[\frac{\delta i_0(f_s)}{i_0(f_s)}+\frac{\delta i_0(f_1-f_2-f_s)}{i_0(f_1-f_2-f_s)}-\frac{r_1}{1+r_1}\frac{\delta r_1}{r_1}+\frac{r_2}{1+r_2}\frac{\delta r_2}{r_2} -\frac{\delta i_0(f_2-f_s)}{i_0(f_2-f_s)}+\frac{R(f_1-f_2-f_s)-R(f_2-f_s)}{R(f_2-f_s)}\right] \quad (14a)$$

with

$$F_z=\frac{1}{m_{zi}\left[\frac{J_1(m_{zi})}{J_0(m_{zi})}+\frac{J_0(m_{zi})-J_2(m_{zi})}{2J_1(m_{zi})}\right]},\ (i=1,2) \quad (14b)$$

and

$$r_1=\left|\frac{i_\pi(f_s)}{i_0(f_s)}\right|, r_2=\left|\frac{i_\pi(f_1-f_2\pm f_s)}{i_0(f_1-f_2\pm f_s)}\right| \quad (14c)$$

with the error transfer factor F_z, the amplitude ratio factor r_1 and r_2. For an error transfer factor smaller than 1, the uncertainty of modulation index will be less than that of heterodyning ratio, whereas for an error transfer factor larger than 1, the uncertainty of modulation index will be amplified and larger than that of heterodyning ratio. As is shown in Fig.7, the error transfer factor F_z is less than 1, while the amplitude factor $r_1/(1+r_1)$ is less than 0.2 and $r_2/(1+r_2)$ is less than 0.9 within the measuring frequency range. According to the specification of ESA, the measured electrical power has an uncertainty of less than 0.1 dB, corresponding to a relative error of 1.15% (=(10.^(0.1/20)-1)×100%) for a single electrical amplitude measurement. According to the specification of PD, the response difference within the 20 MHz frequency difference is no more than 0.15 dB, corresponding to an additional error of 1.74% (=(10.^(0.15/20)-1)×100%) for every heterodyne ratio. Therefore, the measured heterodyning ratio H_z is estimated to have a total error of less than 7.72% (=1.15%×2×0.2+1.15%×2×0.9+1.15%×3+1.74%), indicating a relative error of less than 7.72% delivered to the measured modulation index in the worst case. Besides, the measurement uncertainty as a function of modulation frequency is also included in Fig. 7 for reference.

In the PM measurement, the error dependence of modulation index on the heterodyning ratio H_p can be written as

$$\delta m_p/m_p=F_p\cdot H_p/H_p=F_p\cdot \left[\frac{\delta i_\varphi(f_2-f_1-f_s)}{i_\varphi(f_2-f_1-f_s)}-\frac{\delta i_\varphi(f_2-f_s)}{i_\varphi(f_2-f_s)}+\frac{R(f_1-f_2-f_s)-R(f_2-f_s)}{R(f_2-f_s)}\right] \quad (15a)$$

with

$$F_p=\frac{1}{m_p\left[\frac{J_1(m_p)}{J_0(m_p)}+\frac{J_0(m_p)-J_2(m_p)}{2J_1(m_p)}\right]} \quad (15b)$$

As shown in Fig. 7, the error transfer factor F_p is less than 1 within the measuring frequency range, and the error of the measured modulation index will be less than that of the measured heterodyning ratio H_p. The error of the measured heterodyning ratio is estimated to have an uncertainty of 4.04% (=1.15%+1.15%+1.74%), which means a total relative error of less than 4.04% might be delivered to the measured modulation index in the worst case.

As half-wave voltages of MZM and PM are calculated with the modulation index and microwave driving amplitude, the uncertainty of half-wave voltages will be transferred from not only the modulation index but also microwave driving

This article has been accepted for publication in a future issue of this journal, but has not been fully edited. Content may change prior to final publication. Citation information: DOI 10.1109/JLT.2017.2678978, Journal of Lightwave Technology

amplitude. Therefore, the measured half-wave voltage might have an error of less than 8.87% (=7.72%+1.15%, MZM case) or 5.19% (=4.04%+1.15%, PM case) in the worst case.

In the PD measurement, the uncertainty can be simply derived from the total derivative of Eq. (10) as following

$$\frac{\delta R_f}{R_f} = \frac{\delta i_\varphi(f_1+f_2\pm f_s)}{i_\varphi(f_1+f_2\pm f_s)} - \frac{\delta i_\varphi(f_1-f_2\pm f_s)}{i_\varphi(f_1-f_2\pm f_s)} \quad (16)$$

According to the relative error of less than 1.15% for a single electrical amplitude measurement, the measured frequency response might have a relative error of less than 2.30% (=1.15%+1.15%) in the worst case.

In the LD measurement, the modulation index has an error dependence on the desired frequency components as following

$$\frac{\delta\mu_l}{\mu_l} = \frac{\delta i_\varphi(f_1-f_2-f_s)}{i_\varphi(f_1-f_2-f_s)} - \frac{\delta i_\varphi(f_2-f_s)}{i_\varphi(f_2-f_s)} + \frac{R(f_2-f_s)-R(f_1-f_2-f_s)}{R(f_2-f_s)} \quad (17)$$

which is derived from the total derivative of Eq. (13). Therefore, the total relative error of less than 4.04% (=1.15%+1.15%+1.74%) might be delivered to the extracted modulation index in the worst case.

It is noteworthy that the estimated uncertainty bounds for LD, PD, PM and MZM indicate the measurement uncertainty in the worst case. In the measurement of LDs, PMs and MZMs, the relative error from the ESA and the uneven response of PD can be further reduced by improving the SNR of the desired heterodyning signals and by choosing a better satisfied frequency relationship of $f_1 \approx 2f_2$ or $f_2 \approx 2f_1$. In the PD measurement, we firstly check whether the desired frequency components have enough SNR at the maximum frequency, if yes, then the driving condition will be kept and applied to other lower frequencies. Moreover, as is known, average measurements will reduce the random error. In our measurement, we repeat measurements for nine times and make an average result to reduce random error as much as possible.

Here, we also make a performance comparison between the proposed method and the conventional method including the OSA method and the swept-frequency method for highlighting this work. According to the OSA specification (AQ6370C), the power measurement uncertainty is within 0.4 dB (http://tmi.yokogawa.com/files/uploaded/BUAQ6370SR_10EN_010.pdf). It can be estimated that the OSA method will have an relative error of less than 9.6% (=(10.^(0.8/20)-1)×100%) for MZM, PM and LD cases, while it is 7.72%, 4.04% and 4.04%, respectively, for the MZM, PM and LD case in our method. According to the LCA specification (N4373D), the uncertainty is less than 0.8 dB, from which the measured response for the PD will be no more than 9.6% (=(10.^(0.8/20)-1)×100%), while it is 2.3% with our method.

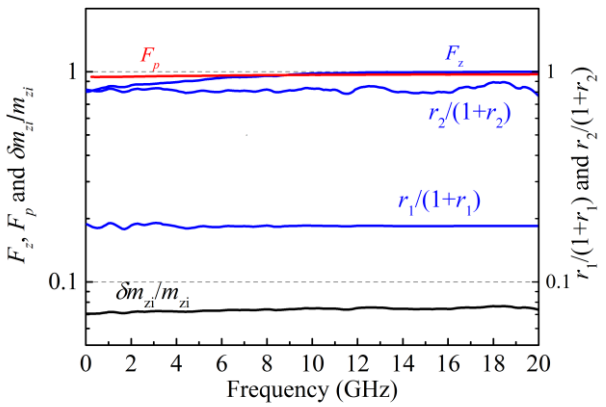

Fig. 7. Error transfer factor, amplitude ratio factor and the measurement error of modulation index m_{zi} at different modulation frequencies in the cases of MZM and PM under test.

V. Discussion and Conclusion

The heterodyne spectrum mapping is essentially an optical microwave mixing. The optical microwave mixing has many applications in ROF systems and other microwave systems for microwave frequency up- or down-conversion. In this work, we add the frequency shifting in the optical mixing, enabling the full mapping from optical spectrum to electrical spectrum for measuring high-speed optoelectronic devices.

In our experiment, all the heterodyning signals show extremely narrow spectrum lines due to inherently mutual coherence between the two optical signals on both branches of the self-heterodyne interferometer originating from the same optical carrier. Our measurement is insensitive to amplitude imbalance and phase difference of the interferometer because it is operated at heterodyne mode instead of interference mode. Our scheme is applicable for different driving levels and operating wavelengths as long as the required frequency relationship is satisfied. Besides, a specially optimized bias phase of MZM is not necessary except in the case of MZM itself under test, since the bias phase has same influence on the desired electrical components. In practice, the larger *cosφ* is recommended for better heterodyne amplitude and SNR, as well as moderate and balanced microwave driving powers.

Our method is capable of extracting absolute frequency responses of MZMs, PMs, PDs and LDs, and it reduces half bandwidth requirement or extends double measuring frequency range, since the frequency response of DUT at *f* is determined from the electrical components at about *f*/2 (MZM, PM and LD cases), or with two driving signals at about *f*/2 (PD case). In contrast to the optical method for measuring MODs, the proposed electrical method achieves very high frequency resolution measurement of the desired optical spectra for MZM, PM and LD, and avoids the line-width influence of laser source due to the nature of self-heterodyne. Compared to the optical methods for measuring PDs, our method provides very narrow linewidth and calibration-free optical stimulus with extremely frequency stability. Different from the VNA method, ours realizes a self-calibrated absolute frequency response measurement for MZMs, PMs, PDs and LDs with same interferometer based on the heterodyne spectrum mapping.

In summary, we have proposed and demonstrated a four-in-one self-calibrated electrical method for microwave characterization of MZMs, PMs, PDs and LDs with a shared self-heterodyne interferometer based on heterodyne spectrum mapping. Frequency responses including the half-wave voltage and chirp parameter of MZM, half-wave voltage of PM,

responsivity of PD, and modulation index of LD at microwave frequencies were extracted with the high-resolution electrical spectrum analysis of optical heterodyne signals. Our method eliminates the need to correct the responsivity fluctuation of other assistant devices in the setup, indicating online measurements of optoelectronic components and photonic integrated circuits.

REFERENCES

[1] J. Capmany and D. Novak, "Microwave photonics combines two worlds," *Nat. Photon.*, vol. 1, no. 6, pp. 319-330, Jun. 2007.

[2] J. Yao, "Microwave photonics," *J. Lightw. Technol.*, vol. 27, no. 3, pp. 314-335, Feb. 1, 2009.

[3] L. Xie, J. W. Man, B. J. Wang, Y. Liu, X. Wang, H. Q. Yuan, L. J. Zhao, H. L. Zhu, N. H. Zhu, and W. Wang, "24-GHz directly modulated DFB laser modules for analog applications," *IEEE Photon. Technol. Lett.*, vol. 24, no. 5, pp. 407-409, Mar. 1, 2012.

[4] Y. Shi, L. Yan and A. Willner, "High-speed electrooptic modulator characterization using optical spectrum analysis," *J. Lightw. Technol.*, vol. 21, no. 10, pp. 2358-2367, Oct. 2003.

[5] N. Courjal, J. M. Dudley, and H. Porte, "Extinction-ratio-independent method for chirp measurements of Mach-Zehnder modulators," *Opt. Exp.*, vol. 12, no. 3, pp. 442-448, Feb. 9, 2004.

[6] S. Oikawa, T. Kawanishi, and M. Izutsu, "Measurement of chirp parameters and halfwave voltages of Mach-Zehnder-type optical modulators by using a small signal operation," *IEEE Photon. Technol. Lett.*, vol. 15, no. 5, pp. 682-684, May, 2003.

[7] H. Kim and A. H. Gnauck, "Chirp characteristics of dual-drive Mach-Zehnder modulator with a finite DC extinction ratio," *IEEE Photon. Technol. Lett.*, vol. 14, no. 3, pp. 298-300, Mar. 2002.

[8] J. E. Bowers and C. A. Burrus, "Optoelectronic components and systems with bandwidths in excess of 26 GHz," *RCA Review*, vol. 46, no. 4, pp. 496-509, Dec. 1, 1985.

[9] P. D. Hale and D. F. Williams, "Calibrated measurement of optoelectronic frequency response," *IEEE Trans. Microwave Theory. Tech.*, vol. 51, no. 4, pp. 1422-1429, Apr. 2003.

[10] X. M. Wu, J. W. Man, L. Xie, Y. Liu, X. Q. Qi, L. X. Wang, J. G. Liu, and N. H. Zhu, "Novel method for frequency response measurement of optoelectronic devices," *IEEE Photon Technol. Lett.*, vol. 24, no. 7, pp. 575-577, Apr. 1, 2012.

[11] A. A. Chtcherbakov, R. J. Kisch, J. D. Bull, and N. A. F. Jaeger, "Optical heterodyne method for amplitude and phase response measurements for ultrawideband electrooptic modulators," *IEEE Photon. Technol. Lett.*, vol. 19, no. 1, pp. 18-20, Jan. 1, 2007.

[12] J. E. Bowers and C. A. Burrus, "Ultra-wide band long-wavelength PIN photodetectors," Invited Paper, *IEEE/OSA J. Lightw. Technol.*, vol. LT-5, no. 10, pp. 1339-1350, Oct. 1, 1987.

[13] R. T. Hawkins, M. D. Jones, S. H. Pepper, and J. H. Go, "Comparison of fast photodetector response measurements by optical heterodyne and pulse response techniques," *J. Lightw. Technol.*, vol. 9, no. 10, pp. 1289-1294, Oct. 1991.

[14] E. Eichen, J. Schlafer, W. Rideout, and J. McCabe, "Wide-bandwidth receiver/photodetector frequency response measurements using amplified spontaneous emission from a semiconductor optical amplifier," *J. Lightw. Technol.*, vol. 8, no. 6, pp. 912-916, Jun. 1990.

[15] D. M. Baney, W. V. Sorin, and S. A. Newton, "High-frequency photodiode characterization using a filtered intensity noise technique," *IEEE Photon. Technol. Lett.*, vol. 6, no. 10, pp. 1258-1260, Oct. 1994.

[16] B. H. Zhang, N. H. Zhu, W. Han, J. H. Ke, H. G. Zhang, M. Ren, W. Li, and L. Xie, "Development of swept frequency method for measuring frequency response of photodetectors based on harmonic analysis," *IEEE Photon. Technol. Lett.*, vol. 21, no. 7, pp. 459-461, Apr. 1, 2009.

[17] M. Yoshioka, S. Sato, and T. Kikuchi, "A method for measuring the frequency response of photodetector modules using twice-modulated light," *J. Lightw. Technol.*, vol. 23, no. 6, pp. 2112-2117, Jun. 2005.

[18] K. Inagaki, T. Kawanishi, and M. Lzutsu, "Optoelectronic frequency response measurement of photodiodes by using high-extinction ratio optical modulator," *IEICE Electron. Exp.*, vol. 9, no. 4, pp. 220-226, Feb. 2012.

[19] T. S. Tan, R. L. Jungerman, and S. S. Elliott, "Optical receiver and modulator frequency response measurement with a Nd:YAG ring laser heterodyne technique," *IEEE Trans. Microw. Theory Tech.*, vol. 37, no. 8, pp. 1217-1222, Aug. 1989.

[20] S. Hou, R. S. Tucker, and T. L. Koch, "High-speed photodetector characterization by delayed self-heterodyne method," *Electron. Lett.*, vol. 25, no. 24, pp. 1632 -1634, Nov. 1989.

[21] N. H. Zhu, J. M. Wen, H. S. San, H. P. Huang, L. J. Zhao, and W. Wang, "Improved optical heterodyne methods for measuring frequency response of photodetectors," *IEEE J. Quantum Electron.*, vol. 42, no. 3, pp. 241-248, Mar. 2006.

[22] T. Dennis and P. D. Hale, "High-accuracy photoreceiver frequency response measurements at 1.55 μm by use of a heterodyne phase-locked loop," *Opt. Exp.*, vol. 19, no. 21, pp. 20103-20114, Oct. 2011.

[23] T. Zhang, N. H. Zhu, B. H. Zhang, and X. Zhang, "Measurement of chirp parameter and modulation index of a semiconductor laser based on optical spectrum analysis," *IEEE Photon. Technol. Lett.*, vol. 19, no. 4, pp. 227-229, Feb. 5, 2007.

[24] N. H. Zhu, T. Zhang, Y. L. Zhang, G. Z. Xu, J. M. Wen, H. P. Huang, Y. Liu, and L. Xie, "Estimation of frequency response of direct modulated lasers from optical spectra," *J. Phys. D, Appl. Phys.* vol. 39, no. 21, pp. 4578-4581, Oct. 20, 2006.

[25] S. J. Zhang, H. Wang, X. H. Zou, Y. L. Zhang, R. G. Lu, and Y. Liu, "Self-calibrating measurement of high-speed electro-optic phase modulators based on two-tone modulation," *Opt. Lett.*, vol. 39, no.12, pp. 3504-3507, Jun. 15, 2014.

[26] S. Zhang,H. Wang, X. Zou, Y. Zhang, R. Lu, H. Li, Y. Liu, "Optical frequency-detuned heterodyne for self-referenced measurement of photodetectors," *IEEE Photon. Technol. Lett.*, vol. 27, no. 9, pp. 1014-1017, May 1, 2015.

[27] S. Zhang, C. Zhang, H. Wang, X. Zou, Y. Zhang, Y. Liu, J. E. Bowers, "Independently self-calibrated frequency response measurements of high-speed modulators and photodetectors with same setup," presented at the Optical Fiber Communication Conf., Anaheim, California, USA, 2016, Paper W4K.2.

[28] G. E. Andrew, R. Askey, and R. Roy, Special Functions, Cambridge University, 2001.

Shangjian Zhang received his BS and MS degree from the University of Electronic Science and Technology of China in 2000 and 2003, respectively, and his PhD degree in 2006 from the Institute of Semiconductors, Chinese Academy of Sciences. He was a visiting researcher at COBRA, Eindhoven University of Technology, the Netherlands. He is a professor at University of Electronic Science and Technology of China. He is presently on sabbatical at University of California, Santa Barbara, USA. Dr. Zhang has authored or coauthored over 100 papers and holds 7 patents. His research interests include high-speed optoelectronic devices and photonic microwave signal processing.

Chong Zhang received the B.S. degree in electrical science and technology from the Harbin Institute of Technology, Harbin, China, in 2007, and the M.S. degree in optical engineering from Zhejiang University, Hangzhou, China, in 2010. He is currently working toward the Ph.D. degree at the University of California, Santa Barbara, CA, USA. His research interests include epitaxial growth of III/V materials on silicon, photonics integration devices on hybrid Silicon platform and applications for high speed optical interconnection.

Heng Wang received his BS from the School of Science, Changchun University of Science and Technology, in 2012. He is currently a Ph.D student at University of Electronic Science and Technology of China. His research interests include high-speed optoelectronic devices.

Xinhai Zou received his BS in 2011 from the Chongqing University of Posts and Telecommunications, and his MS degree from the University of Electronic Science and Technology of China in 2014. He is currently a Ph.D student in the School of Optoelectronic Information at University of Electronic Science and Technology of China. His research interests include high-speed optical signal processing.

Yali Zhang received her BS and MS from the Xi'an Jiaotong University in 2002 and 2005, respectively, and her PhD degree from the Institute of Semiconductors, Chinese Academy of Sciences. She is currently an associate professor in the School of Optoelectronic Information at University of Electronic Science and Technology of China. Her research interests include optical communications and integrated optics and microwave photonics.

Yong Liu received his BS and MS from the University of Electronic Science and Technology of China in 1991 and 1994, respectively, and his PhD degree from the Eindhoven University of Technology. He is currently a professor at University of Electronic Science and Technology of China. His research interests include optical communications and integrated optics and microwave photonics.

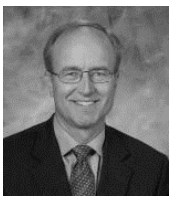

John E. Bowers holds the Fred Kavli Chair in Nanotechnology, and is the Director of the Institute for Energy Efficiency and a Professor in the Departments of Electrical and Computer Engineering and Materials at University of California, Santa Barbara (UCSB). He is a cofounder of Aurrion, Aerius Photonics and Calient Networks. Dr. Bowers received his M.S. and Ph.D. degrees from Stanford University and worked for AT& Bell Laboratories and Honeywell before joining UCSB. Dr. Bowers is a member of the National Academy of Engineering and a fellow of the IEEE, OSA and the American Physical Society. He is a recipient of the OSA/IEEE Tyndall Award, the OSA Holonyak Prize, the IEEE LEOS William Streifer Award and the South Coast Business and Technology Entrepreneur of the Year Award. He and coworkers received the EE Times Annual Creativity in Electronics (ACE) Award for Most Promising Technology for the heterogeneous silicon laser in 2007. Bowers' research is primarily in optoelectronics and photonic integrated circuits. He has published 10 book chapters, 600 journal papers, 900 conference papers and has received 54 patents.